Probing sub-pc massive binary black holes through microlensing of lensed QSOs

闫昌硕 (Yan, Chang-shuo)
NAOC
2015.2.9 Taiwan

collaborators：Youjun Lu
Qingjuan Yu
Shude Mao
Joachim Wambsganss

Massive binary black holes

- Many or most galaxies house massive black holes
- Λ CDM cosmology: hierarchal mergers
- Observation:
- double-peaked emission lines: dual AGNs
    - separation is large: mutual orbital speeds are small compared to the width of emission lines
    - separation is small enough to produce a larger orbital velocity: the emission line regions of the two will overlap
- X-ray image/ optical image/ radio image

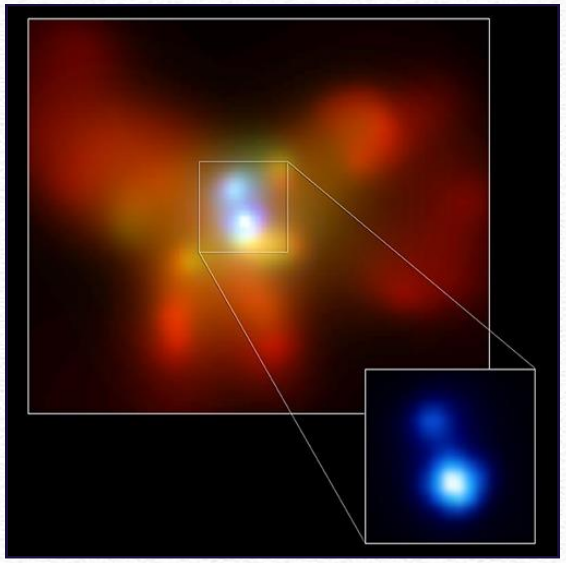

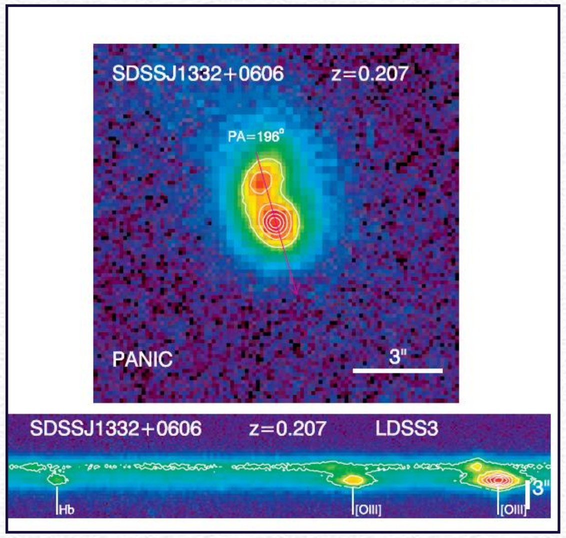

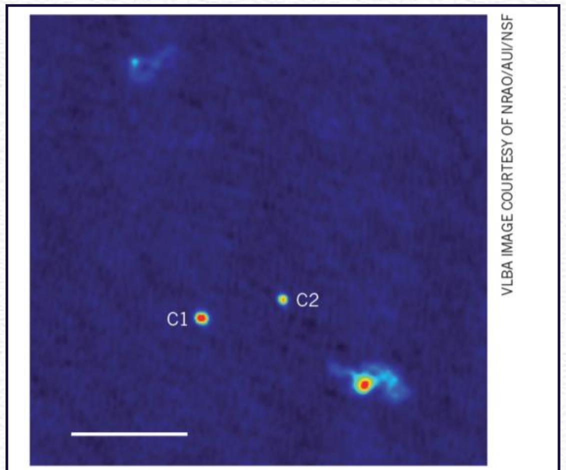

Figure 1 | A tight binary. A radio image of the binary supermassive black hole system 0402+379,

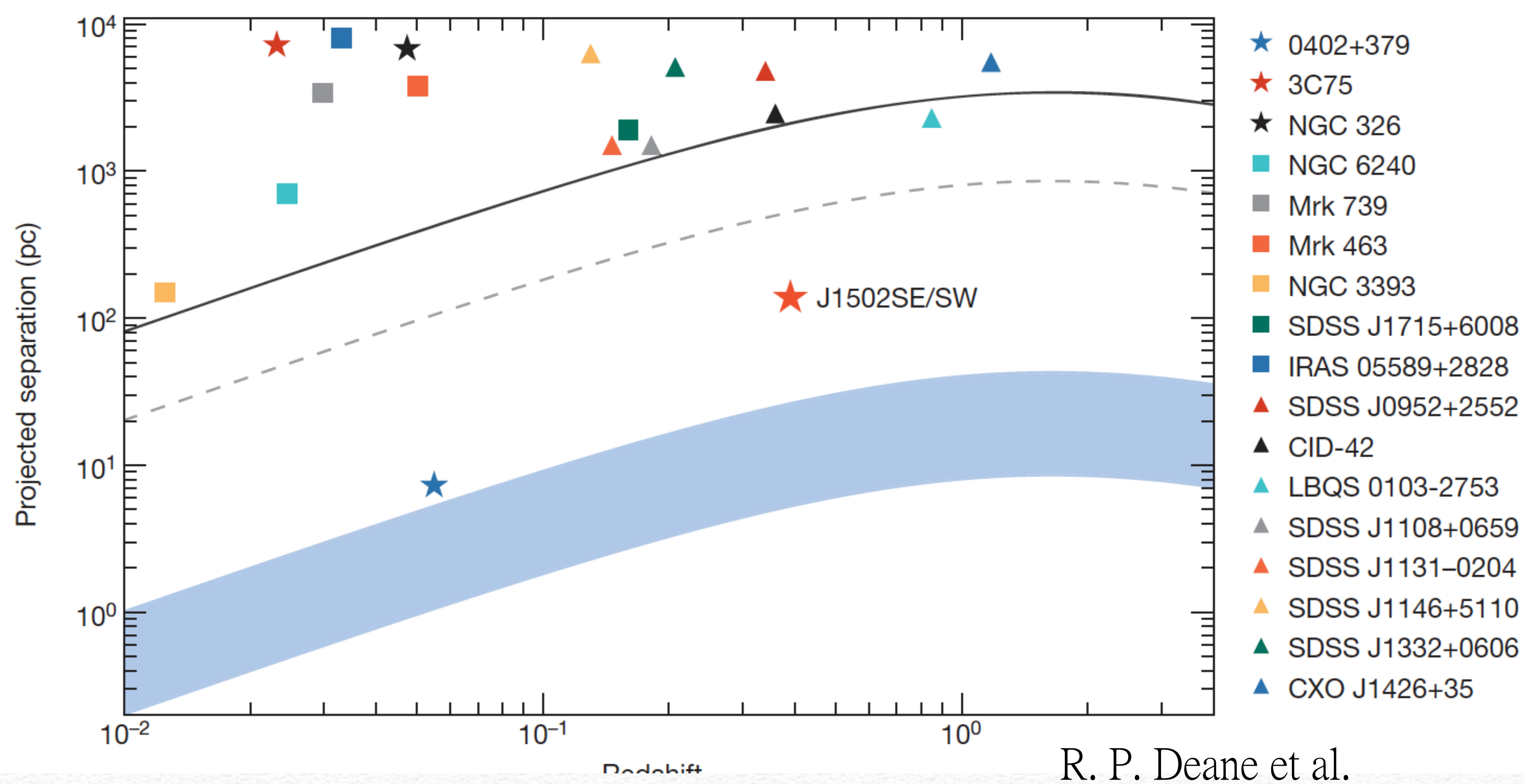

Figure 2 | Dual/binary AGN confirmed or discovered with direct imaging. Sample of binary/dual AGN confirmed or discovered by direct imaging at X-ray (squares), optical/infrared (triangles) and radio (stars) wavelengths. Typical spatial resolution limits of Chandra, the Hubble Space Telescope (HST) and VLBI are indicated by the solid and dashed lines, and shaded blue area, respectively. This illustrates that high-angular-resolution radio observations are able to survey a significantly larger cosmological volume for binary AGN with separations comparable to the black hole gravitational spheres of influence (<10 pc for $M_{BH} \approx 10^8 M_{\odot}$).

R. P. Deane et al.

- sub-pc scale: hard to be detected:

- double-peaked broad lines (Alternative explanation : from eccentric discs) /asymmetric broad line profile or offset broad line emission (orbital motion of massive sub-pc BBHs but also may be from a recoil BHs)

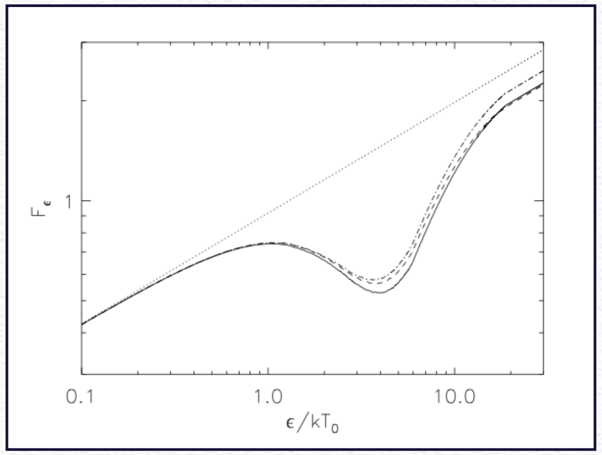

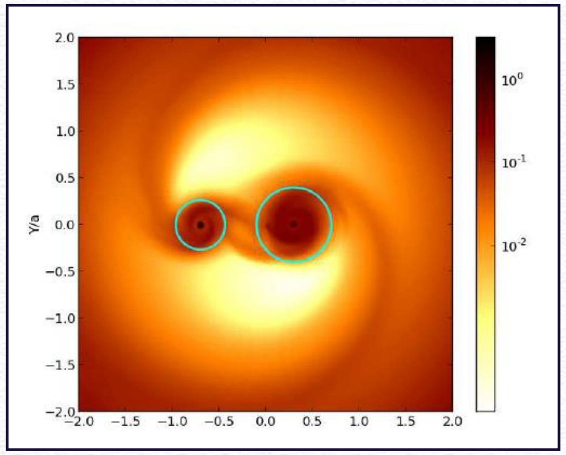

- periodical variation of the QSO light curves etc.

- gap opened: SED signature:

- Gravitational Wave

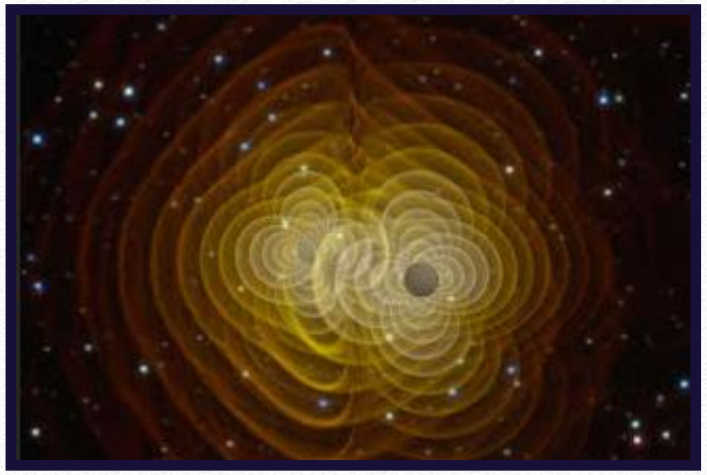

GAP

surface brightness

width of the gap: $2a_{\rm BBH}(q/3)^{1/3}$

$$R_{\rm RL}(x) = 0.49a_{\rm BBH}x^{2/3}/[0.6x^{2/3} + \ln(1+x^{1/2})].$$

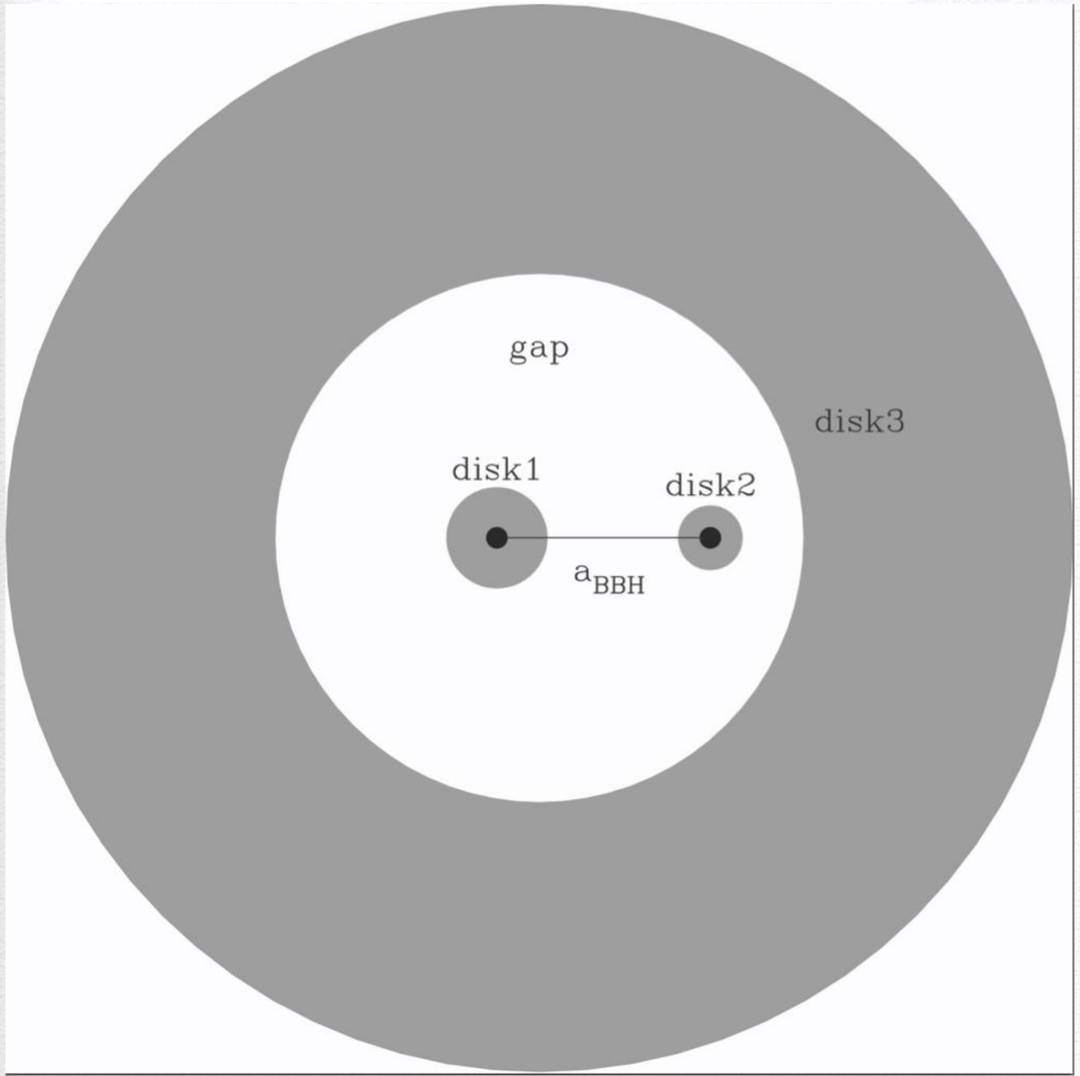

Thin accretion disk

$$T(r) = \left(\frac{3GM_\bullet \dot{M}_\bullet}{8\pi\sigma r_{in}^3}\right)^{1/4} \left(\frac{r_{in}}{r}\right)^{3/4} \left(1 - \sqrt{\frac{r_{in}}{r}}\right)^{1/4}$$

$$\boxed{r_{1/2}} = 2.44\left[\frac{45G^2M_{\rm BH}^2 m_p f_{\rm Edd}\lambda^4}{4\pi^5 h_P c^3 \sigma_T \eta}\right]^{1/3}\sqrt{\cos i}$$

$$= 1.68\times 10^{16}{\rm cm}\left(\frac{M_{\rm BH}}{10^9 M_\odot}\right)^{2/3}\left(\frac{f_{\rm Edd}}{\eta}\right)^{1/3}\boxed{\left(\frac{\lambda}{\mu{\rm m}}\right)^{4/3}}$$

TABLE 1
PARAMETERS FOR DIFFERENT SYSTEMS

Model	$M_\bullet$	q	$f_{\rm E,1}$	$f_{\rm E,2}$	$f_{\rm E,c}$	$a_{\rm BBH}(r_g)$
S0	$10^8M_\odot$	...	...	...	0.3	...
B1	$10^8M_\odot$	0.25	0.3	0.01	0.242	500
B2	$10^8M_\odot$	0.25	0.3	0.01	0.242	1000
B3	$10^8M_\odot$	0.25	0.3	0.01	0.242	2000
B4	$10^8M_\odot$	0.25	0.3	0.01	0.242	3000
B5	$10^8M_\odot$	0.25	10^{-4}	0.3	0.06	500
B6	$10^8M_\odot$	0.25	0.3	0.3	0.3	500
B7	$10^8M_\odot$	1.0	0.3	0.3	0.3	500
B8	$10^8M_\odot$	0.1	10^{-4}	0.3	0.027	500

SED

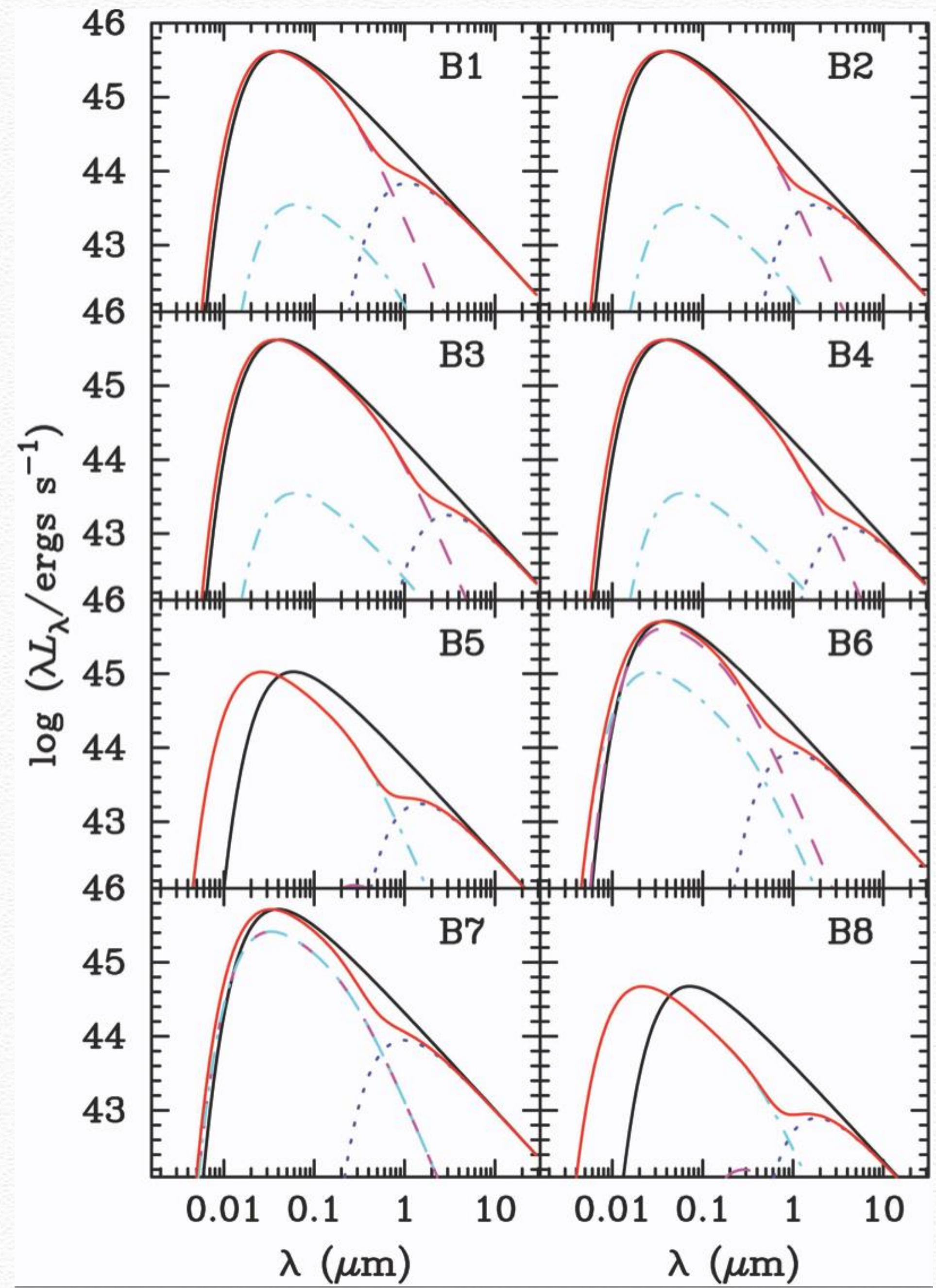

Micro-lensing: probing the structure of the accretion disk

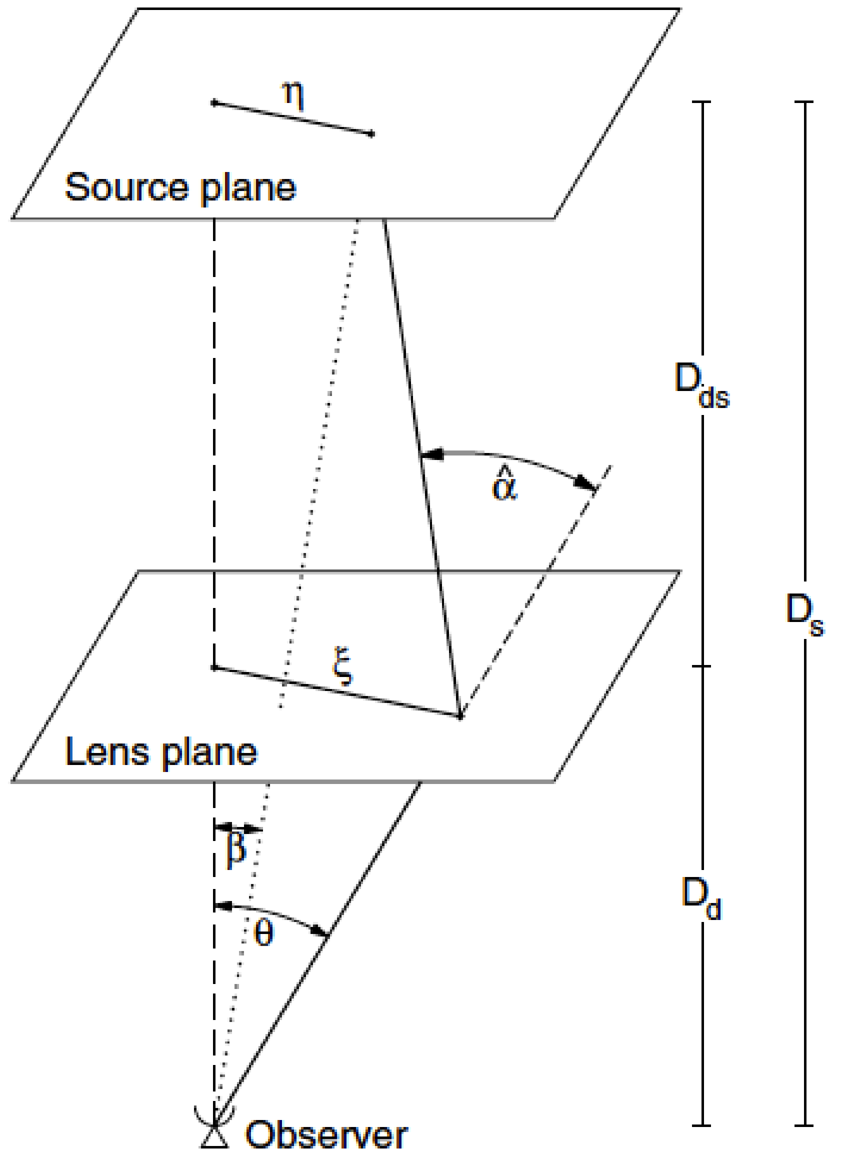

Fig. 12. Sketch of a typical gravitational lens system

$$\langle\theta_{\rm E}\rangle = D_{OS}\left(\frac{4G\langle M\rangle}{c^2 D_{OL}}\frac{D_{LS}}{D_{OS}}\right)^{1/2} = (1.54\times10^{17})\left(\frac{\langle M\rangle}{M_\odot}\right)^{1/2} h^{-1}\ {\rm cm},$$

non-singular isothermal sphere lens

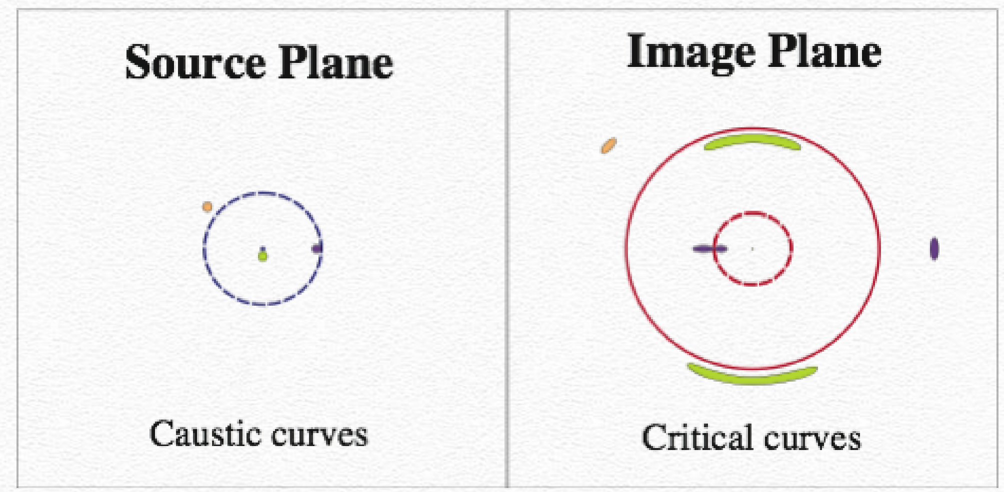

non-singular isothermal ellipsoid lens

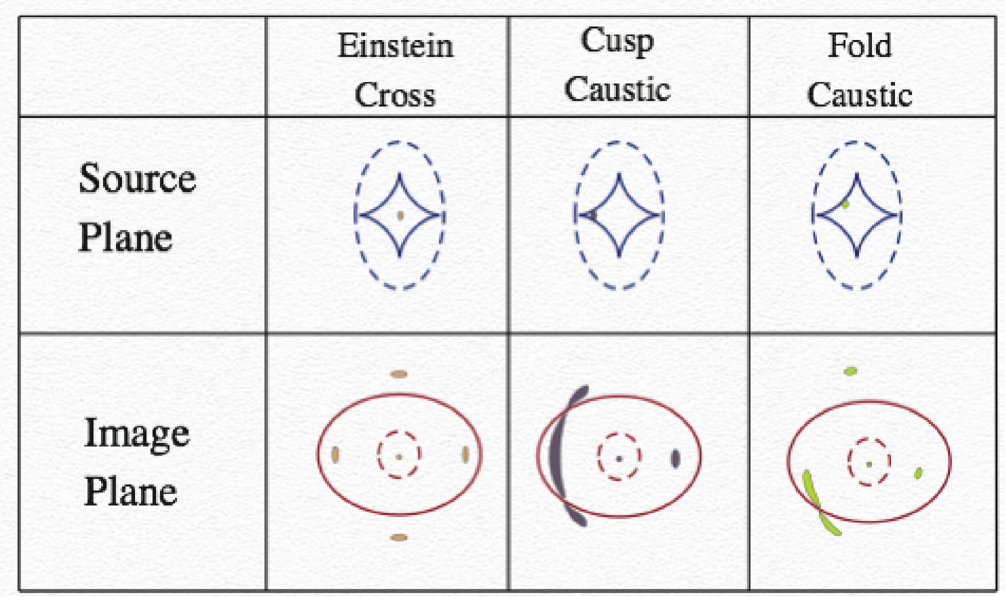

Credit: A. Amara & T. Kitching

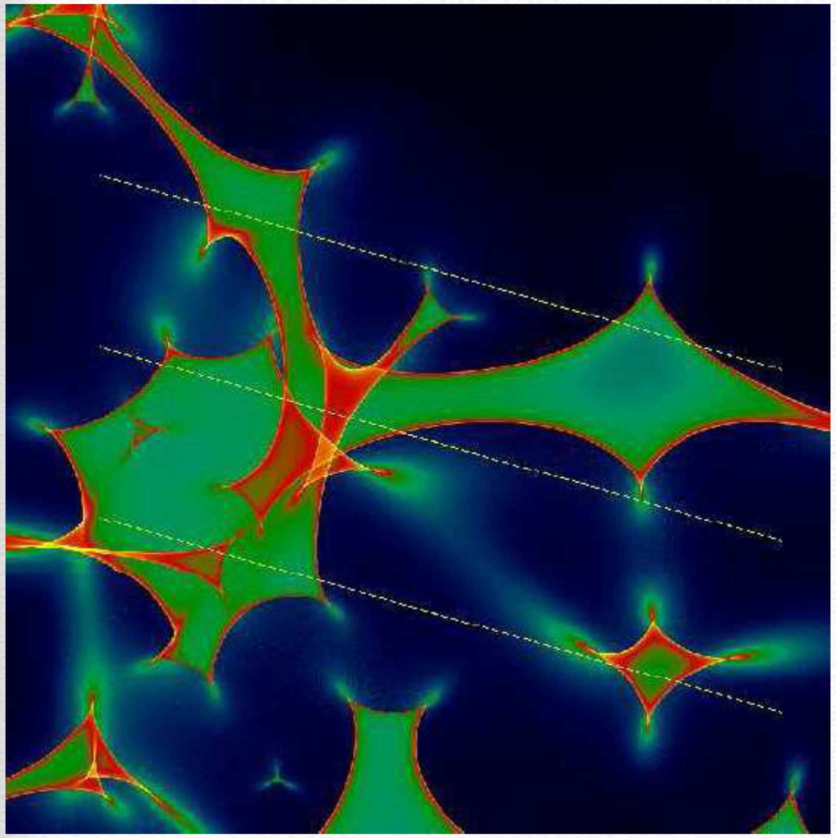

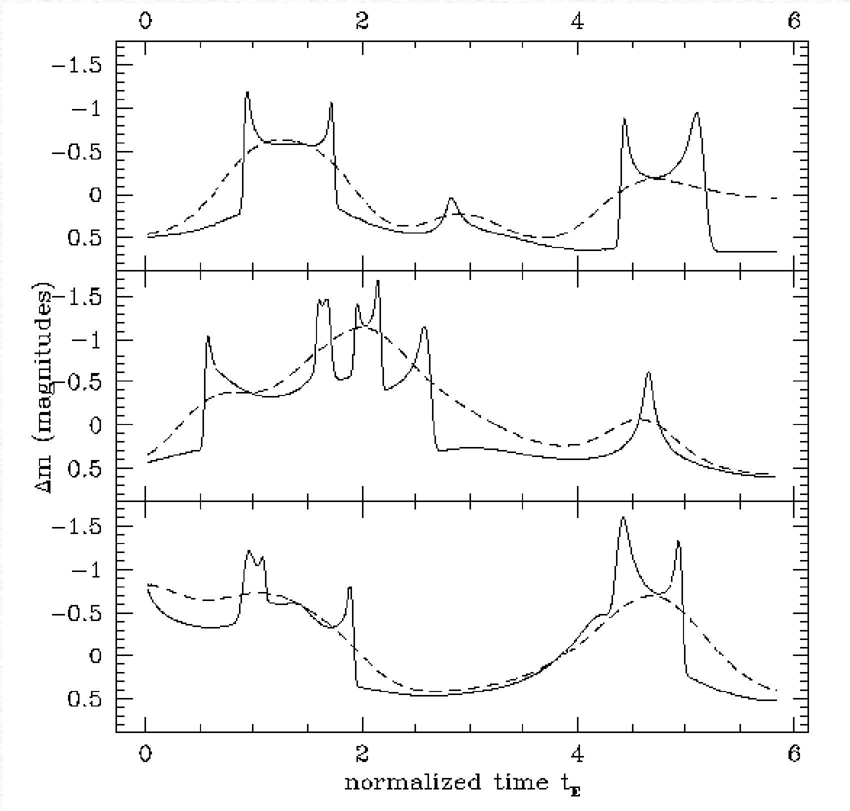

Micro-lensing lightcurves: probe the scale of the accretion disk

Wambsganss 2006

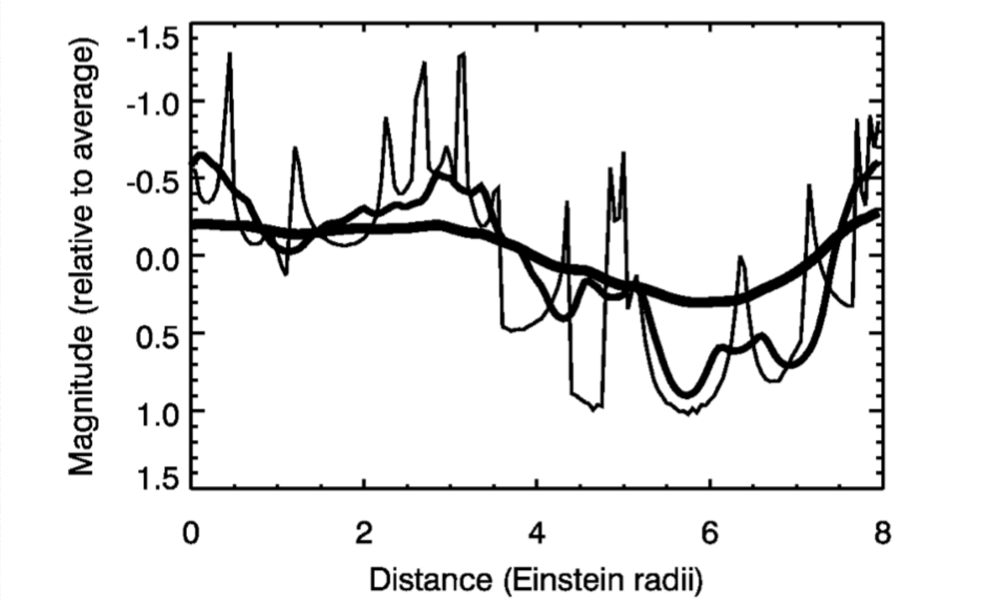

FIG. 4.—Sample light curves from the positive-parity magnification map in Fig. 2 and both maps in Fig. 3 ($\kappa = \gamma = 0.4$). The source travels on a vertical path of length $4r_E$ in the center of each map (Fig. 2, *top, black line*). The thin curve is from the unconvolved positive-parity map, the medium curve is from the convolution with the disk viewed in the filter associated with the peak surface brightness at the maximum temperature T_0 ($i = 0$), and the thick curve is from the convolution in the filter that is a factor of 7.44 longer in wavelength ($i = 10$).

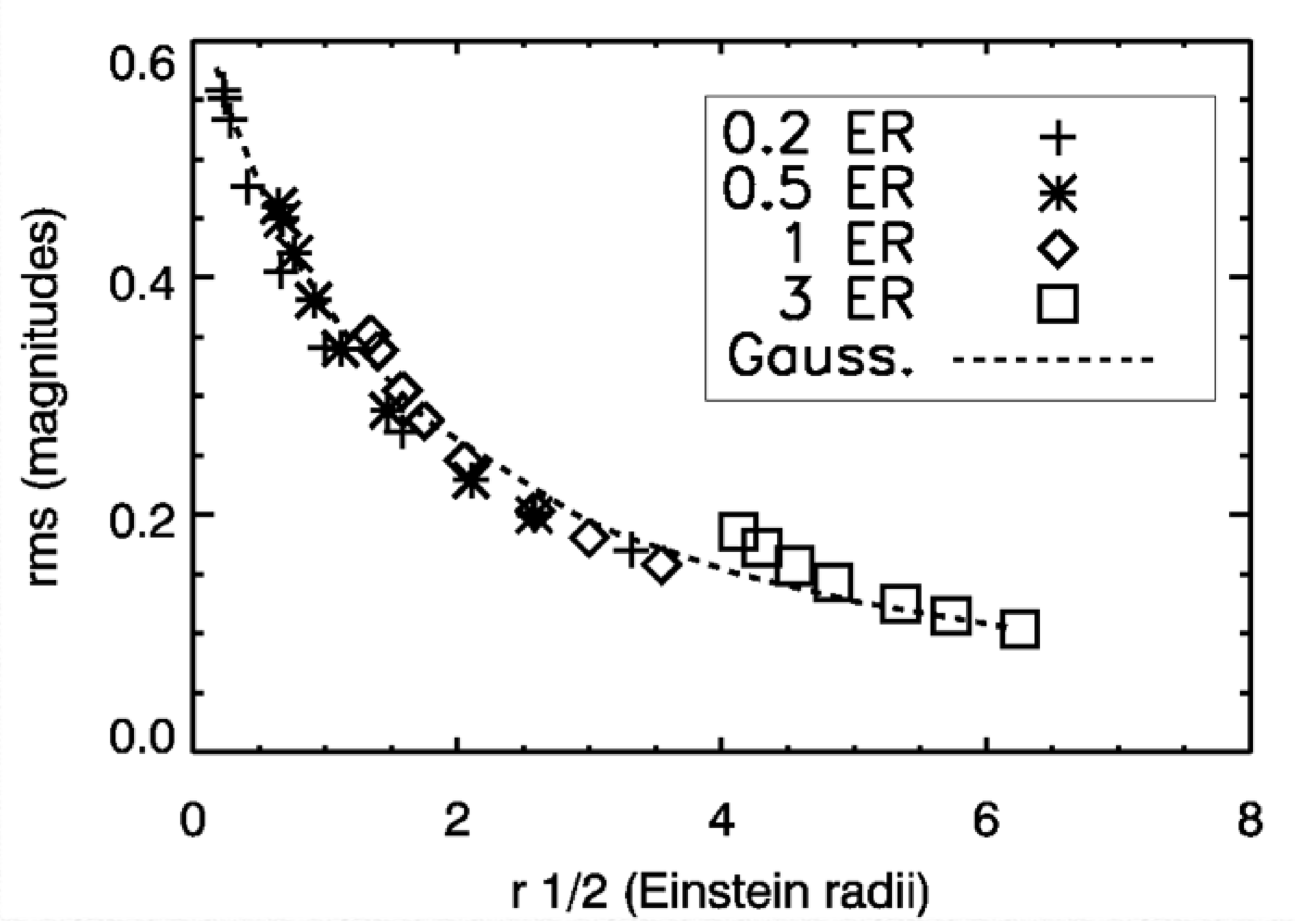

Mortonson &Schechter 2005

A general method for analyzing the light curves of microlensed quasars

Kochanek et al. 2004

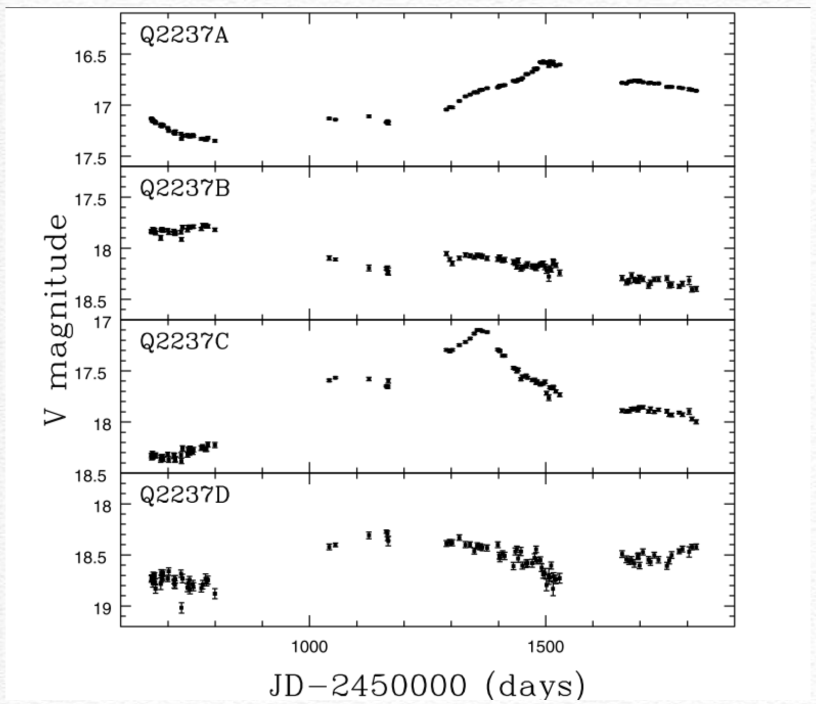

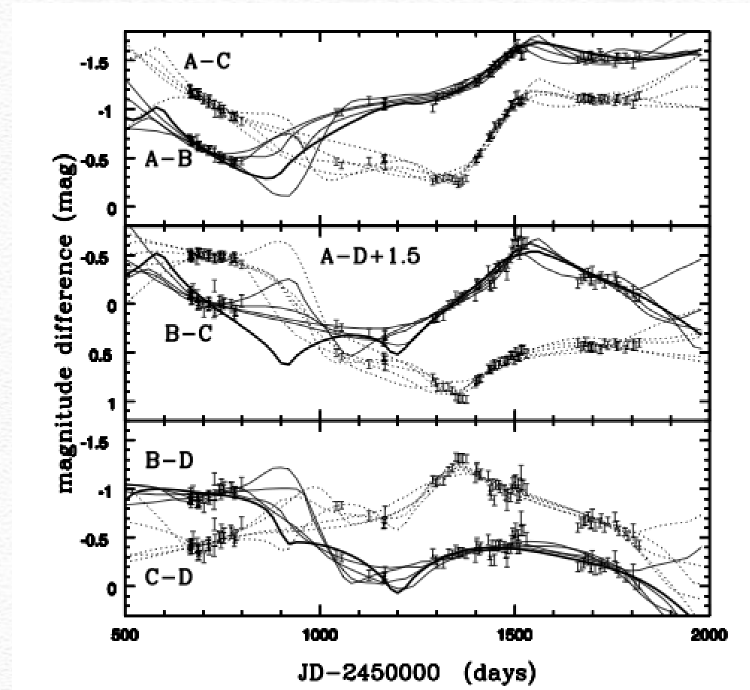

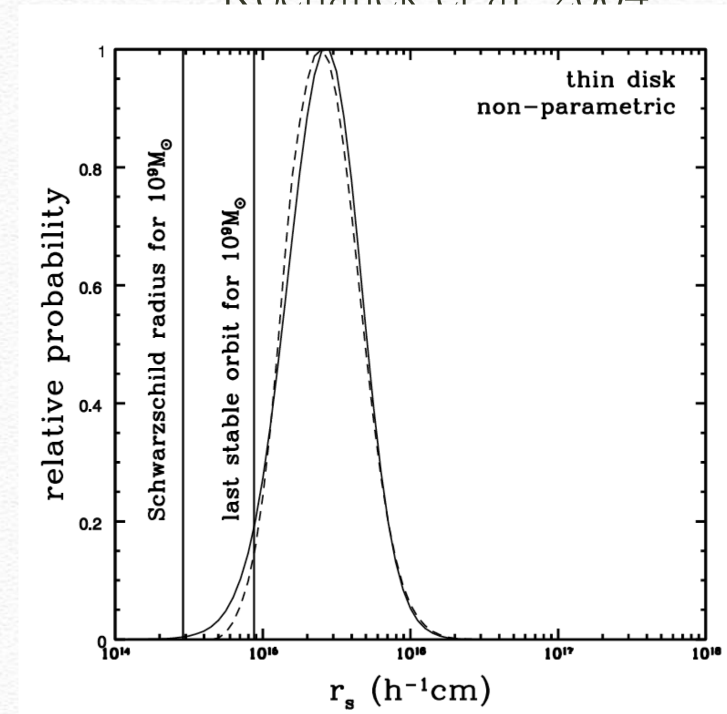

Using the Bayesian theorem, the posterior probability distribution of the parameters involved in the fitting for a given set of data {D} is

$$\chi^2 = \sum_i \frac{(\delta m_i - \delta m_i')^2}{\sigma_i^2 + \sigma_1^2},$$

$$P(D|\hat{r}_s, \kappa_*, \hat{v}_e, \xi_t) = P(\chi^2) \propto \Gamma\left[\frac{N_{\rm dof}-2}{2}, \frac{\chi^2}{2f_0^2}\right], \quad (11)$$

$$P(\hat{r}_s, \kappa_*, \hat{v}_e, \xi_t|D) \propto P(D|\hat{r}_s, \kappa_*, \hat{v}_e, \xi_t) P(\hat{r}_s) P(\kappa_*) \times P(\hat{v}_e) P(\xi_t), \quad (10)$$

Methods

- Binary black hole: Mock light curves
- Single black hole: fit the light curves
- Parameter estimation

TABLE 1
PARAMETERS FOR DIFFERENT SYSTEMS

Model	$M_\bullet$	q	$f_{E,1}$	$f_{E,2}$	$f_{E,c}$	$a_{BBH}(r_g)$
S0	$10^8 M_\odot$	...	...	...	0.3	...
B1	$10^8 M_\odot$	0.25	0.3	0.01	0.242	500
B2	$10^8 M_\odot$	0.25	0.3	0.01	0.242	1000
B3	$10^8 M_\odot$	0.25	0.3	0.01	0.242	2000
B4	$10^8 M_\odot$	0.25	0.3	0.01	0.242	3000
B5	$10^8 M_\odot$	0.25	10^{-4}	0.3	0.06	500
B6	$10^8 M_\odot$	0.25	0.3	0.3	0.3	500
B7	$10^8 M_\odot$	1.0	0.3	0.3	0.3	500
B8	$10^8 M_\odot$	0.1	10^{-4}	0.3	0.027	500

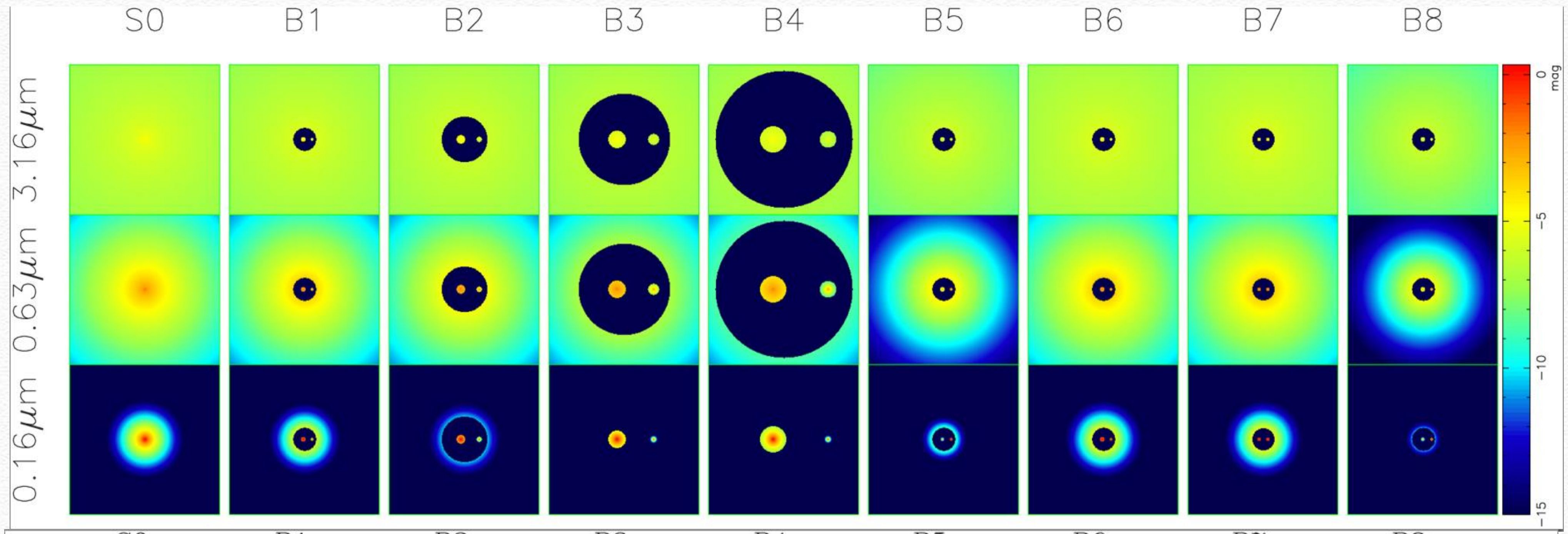

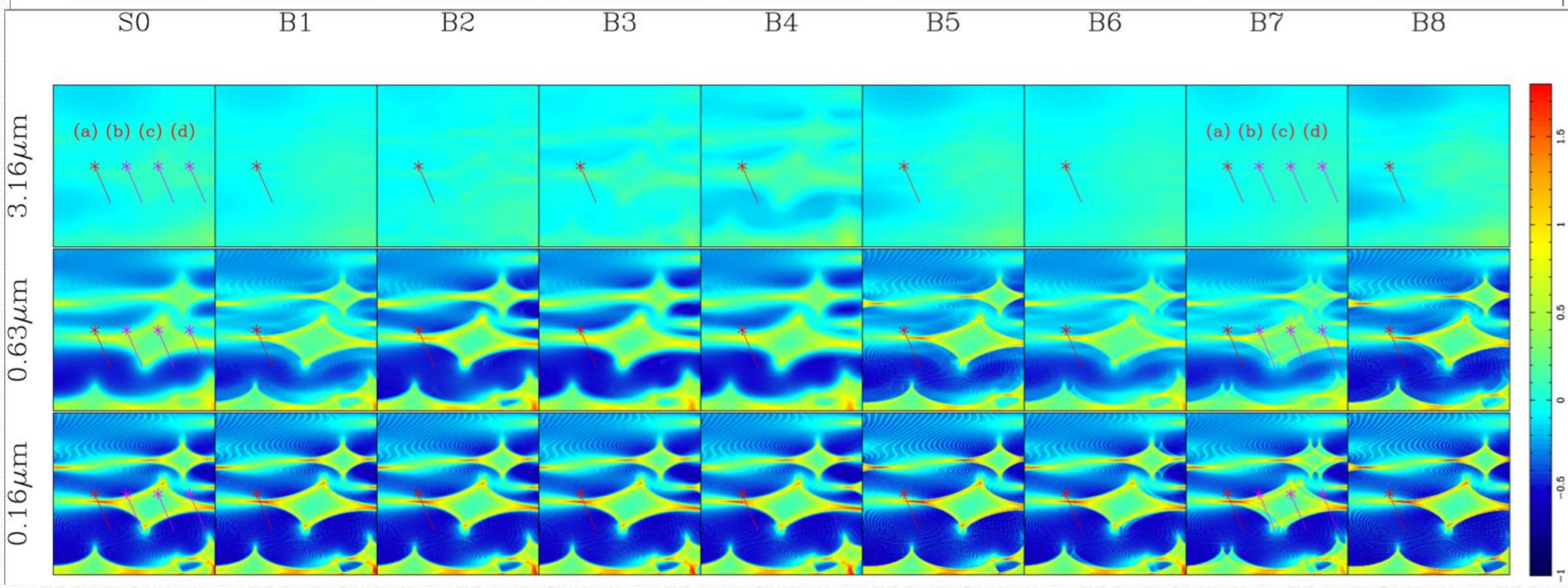

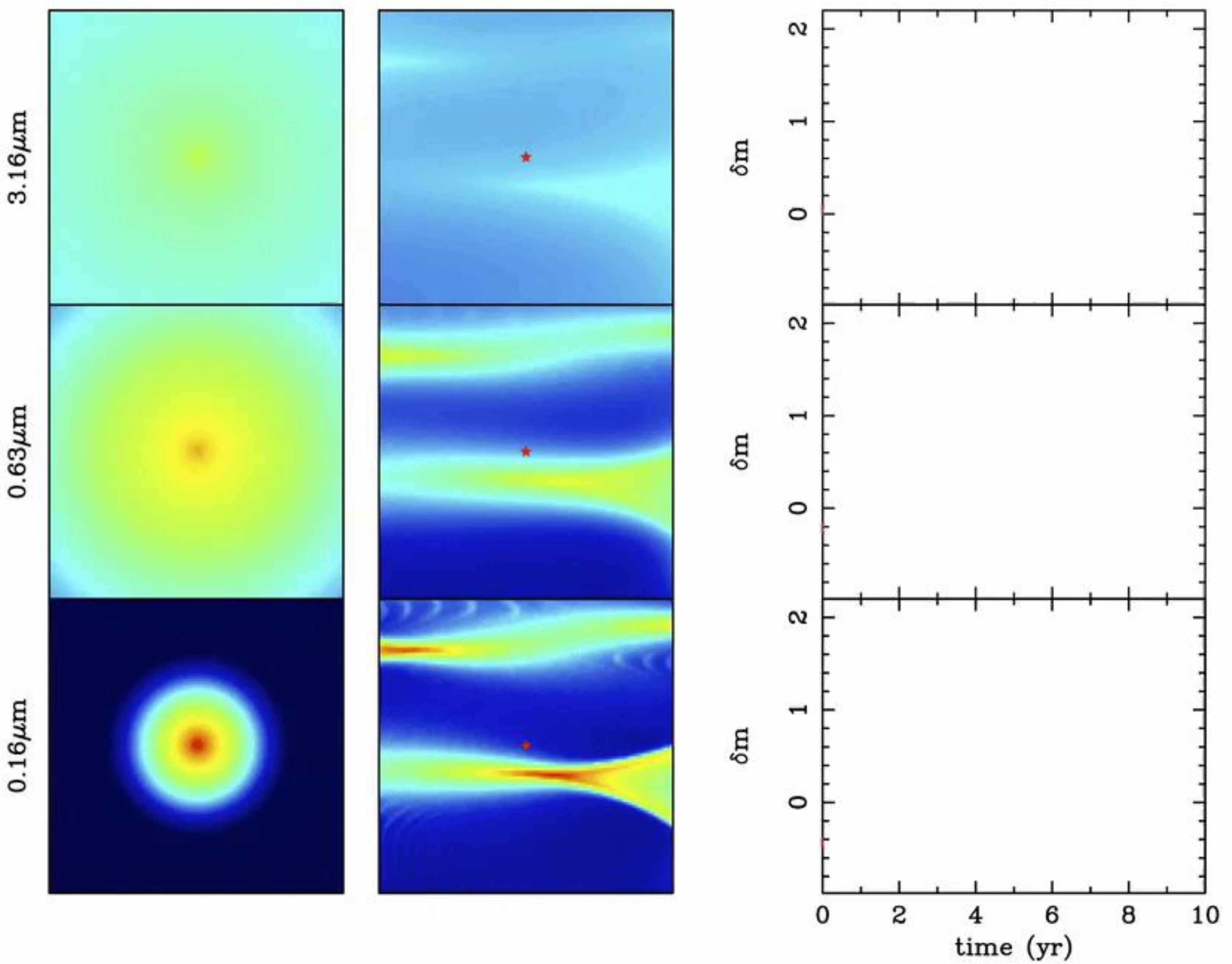

3.16μm
0.63μm
0.16μm
δm
0
1
2
0
2
4
6
8
10
time (yr)

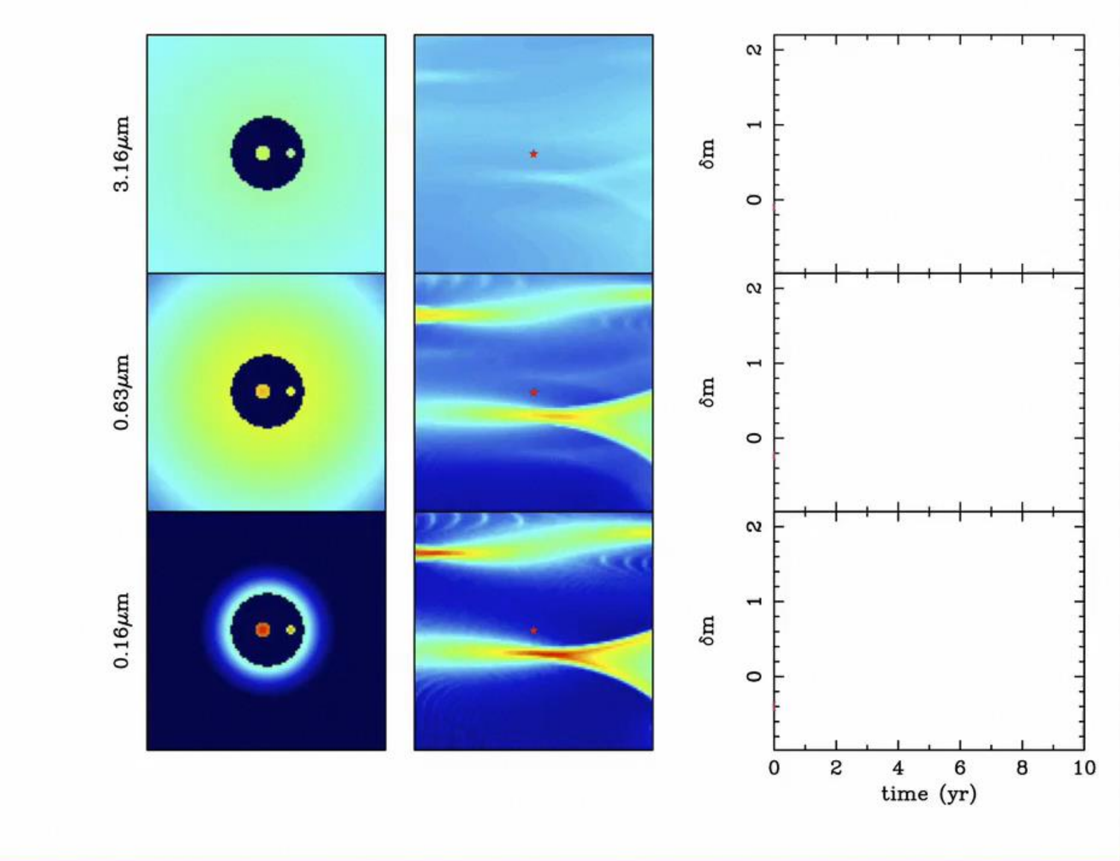

q=0.25
aBBH=500Rg
fedd1=0.3
fedd2=0.01

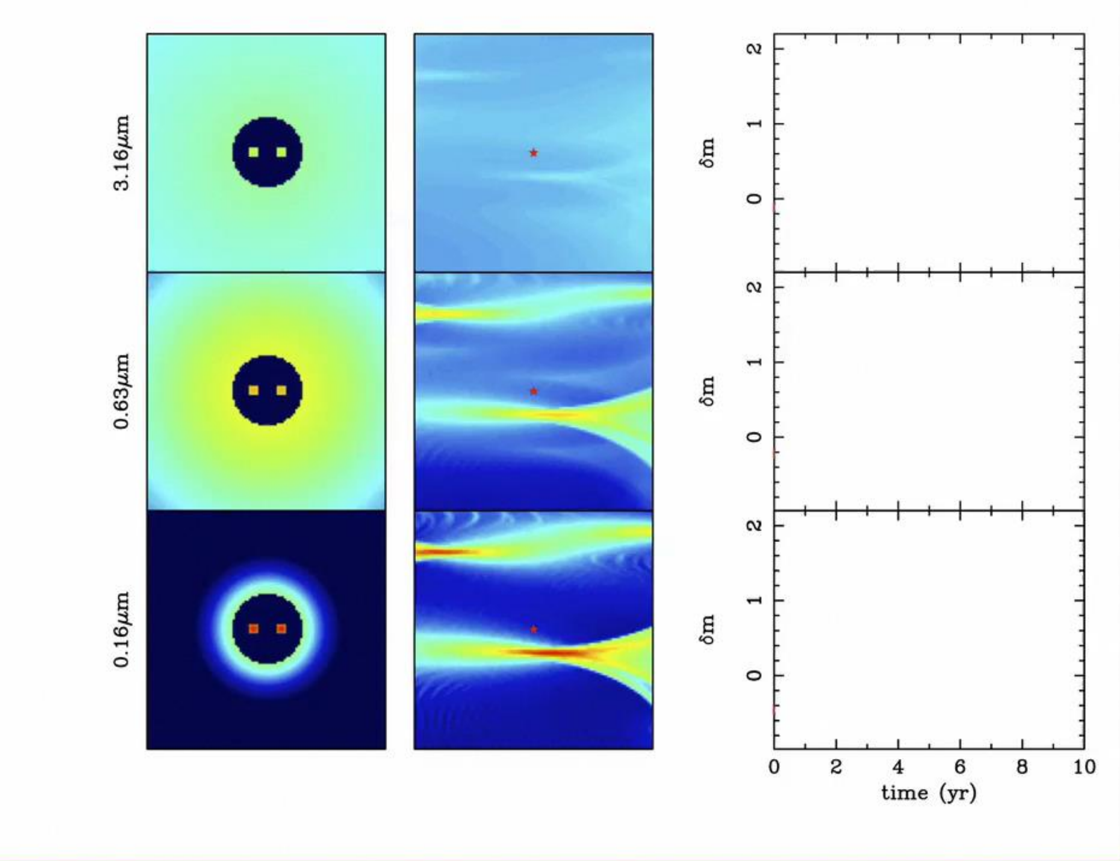

q=1.0
aBBH=500Rg
fedd1=0.3
fedd2=0.3

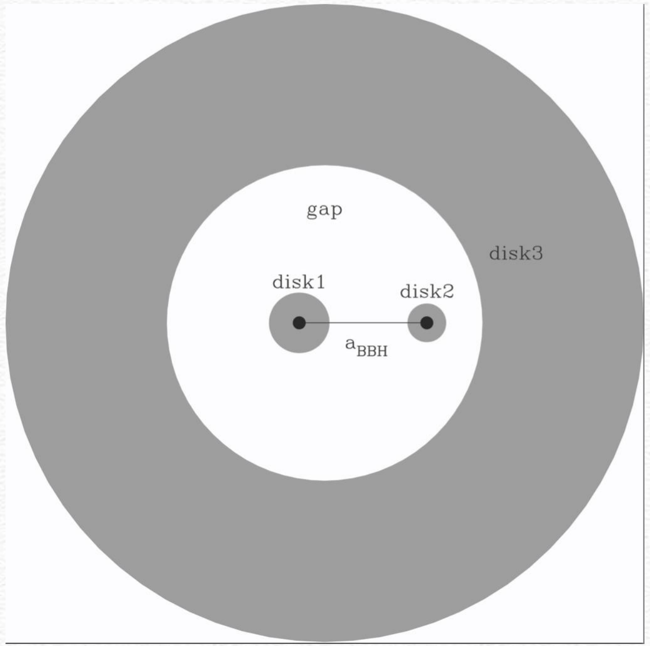

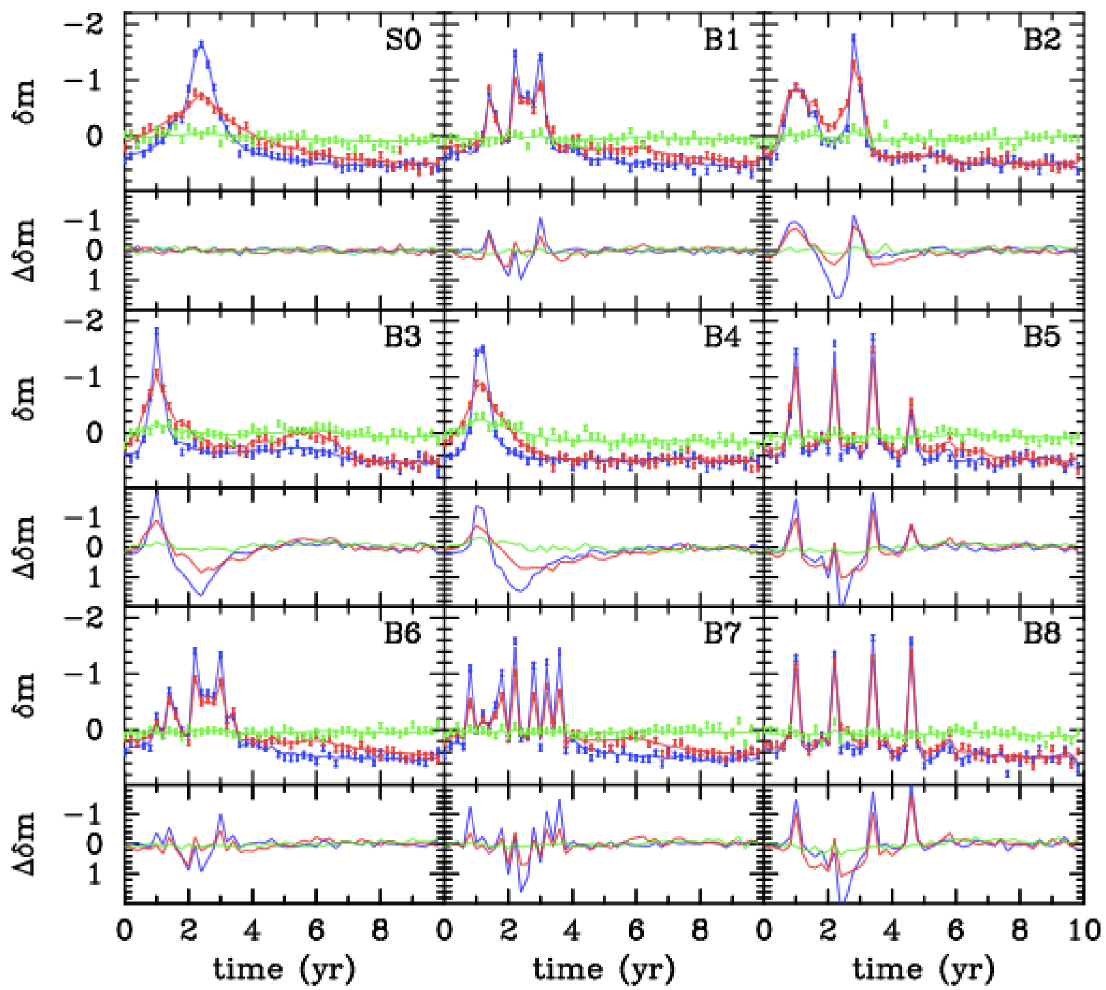

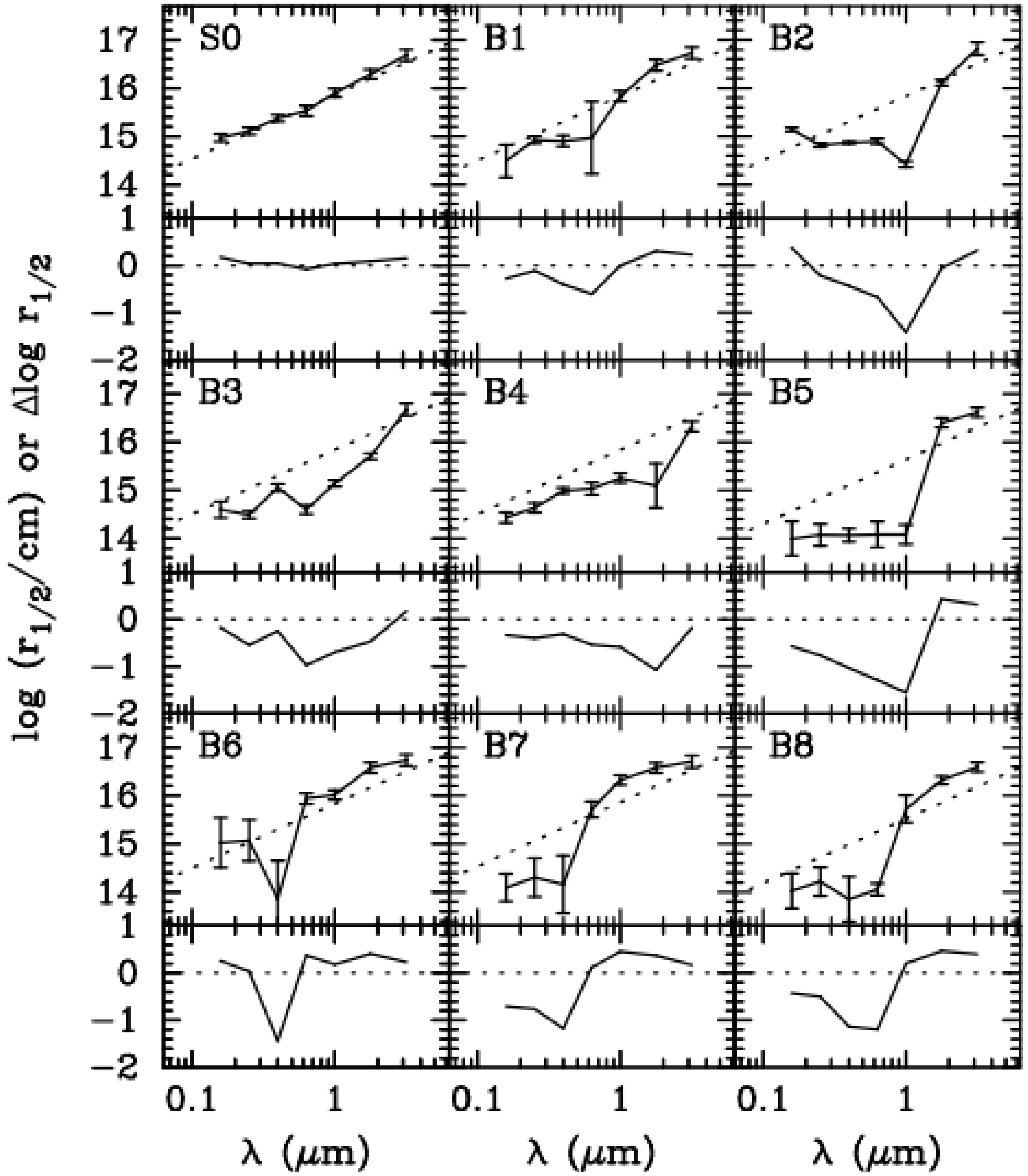

rotating case

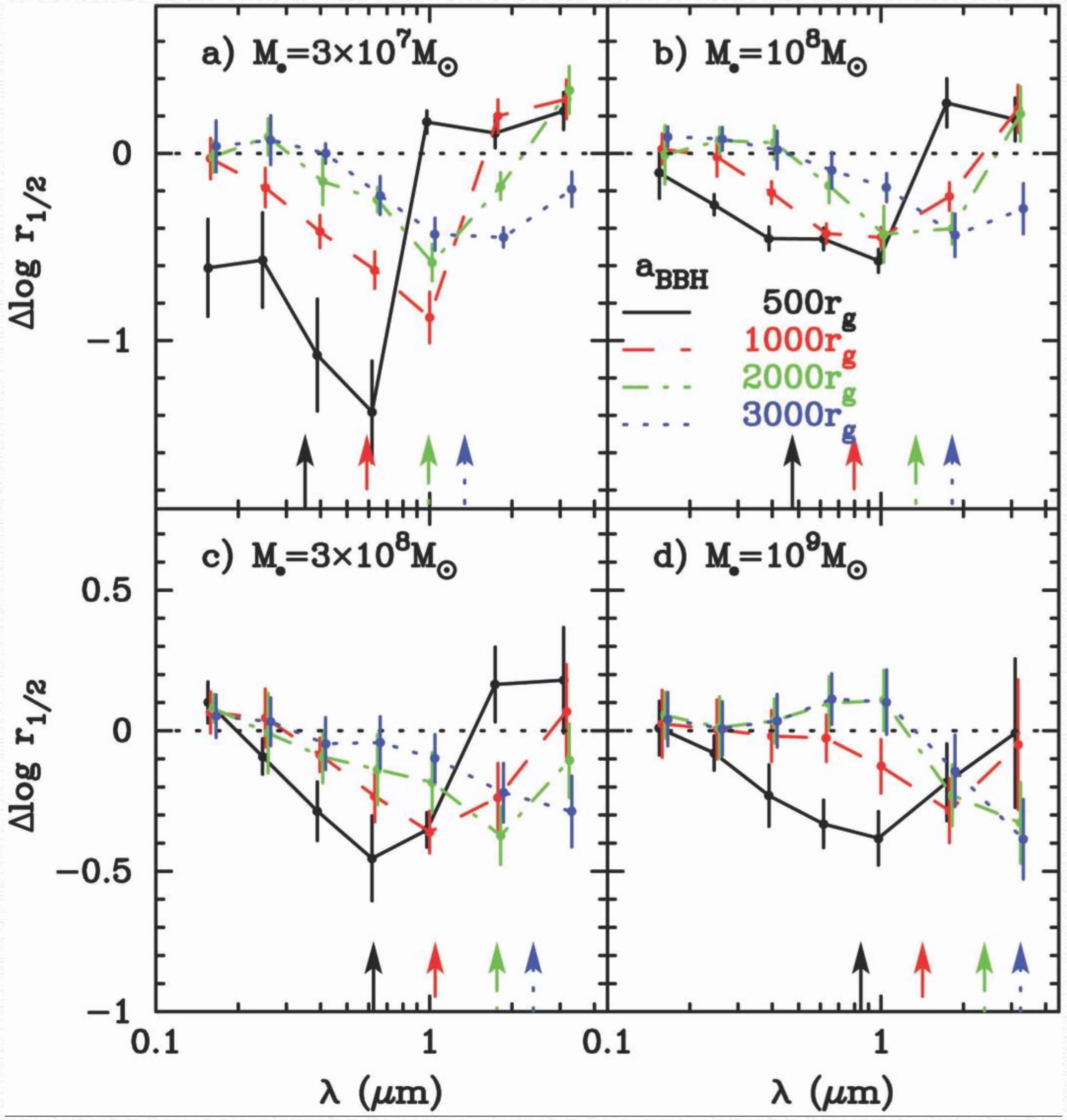

The $r_{1/2} - \lambda$ residual is more prominent for BBH systems with smaller aBBH, and the wavelength of the dip in the $r_{1/2} - \lambda$ residual increases with increasing a_{BBH}.

Summary

- The microlensing light curves of a BBH QSO system can be significantly different from that of a single MBH QSO system because of the existence of the gap and the rotation of the BBH and its associated small disks around the mass center.

- The estimated half-light radius-wavelength relations of BBH QSO systems can be much flatter than that of single MBH QSO systems at a wavelength range determined by the BBH parameters, such as the total mass, mass ratio, separation, etc., which is primarily due to the existence of the gap.

- The unique microlensing feature of BBH QSO systems can be used to select and probe sub-pc BBHs in a large number of lensed QSOs that will be discovered in the near future.(LSST, Pan-STARRS, Euclid, etc.)

- The occurrence of BBHs in lensed QSOs should be in the range of a few thousandth to a few percent. The total number of currently known lensed QSOs is 100 so several of these lensed QSOs could host BBH systems with separation 1000rg, which may be detectable through the microlensing event(s).

A new method to probe the sub-pc binary black holes

THANK YOU !